IEEE Photonics Journal
An IEEE Photonics Society Publication

Nondegenerate Four-Wave Mixing in a Dual-Mode Injection-Locked InAs/InP(100) Nanostructure Laser

Volume 6, Number 1, February 2014

Cheng Wang
Frédéric Grillot
Fan-Yi Lin
Ivan Aldaya
Thomas Batte
Christophe Gosset
Etienne Decerle
Jacky Even

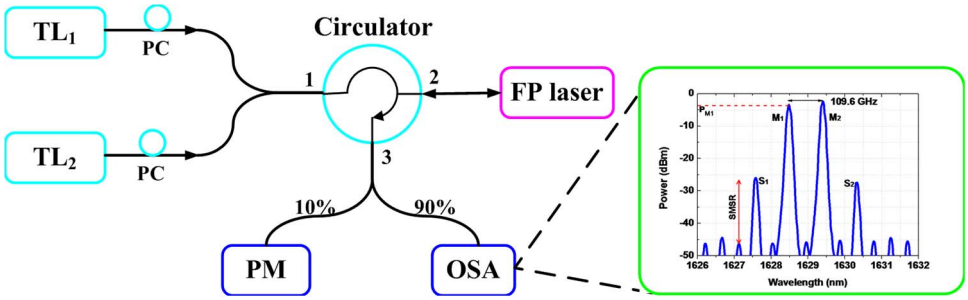

DOI: 10.1109/JPHOT.2013.2295473
1943-0655 © 2013 IEEE

Nondegenerate Four-Wave Mixing in a Dual-Mode Injection-Locked InAs/InP(100) Nanostructure Laser

Cheng Wang,[1,2] Frédéric Grillot,[1] Fan-Yi Lin,[3] Ivan Aldaya,[1,4] Thomas Batte,[2] Christophe Gosset,[1] Etienne Decerle,[5] and Jacky Even[2]

[1]Télécom ParisTech, Ecole Nationale Supérieure des Télécommunications, CNRS LTCI, 75634 Paris Cedex 13, France
[2]Université Européenne de Bretagne, Laboratoire CNRS FOTON, INSA, 35043 Rennes Cedex, France
[3]Institute of Photonics Technologies, Department of Electrical Engineering, National Tsing Hua University, Hsinchu 300, Taiwan
[4]Instituto Tecnológico y de Estudios Speriores de Monterrey, Monterrey, Mexico
[5]Yenista Optics, 4 rue Louis de Broglie, 22300 Lannion Cedex, France

DOI: 10.1109/JPHOT.2013.2295473

Manuscript received November 8, 2013; revised December 10, 2013; accepted December 11, 2013. Date of publication December 20, 2013; date of current version January 3, 2014. The work of F. Grillot was supported by the European Office of Aerospace Research and Development (EOARD) under Grant FA8655-12-1-2093. The work of C. Wang was supported by the China Scholarship Council. Corresponding author: C. Wang (e-mail: cheng.wang@insa-rennes.fr).

Abstract: The nondegenerate four-wave mixing (NDFWM) characteristics in a quantum-dot Fabry–Perot laser are investigated, employing the dual-mode injection-locking technique. The solitary laser features two lasing peaks, which provides the possibility for efficient FWM generation. Under optical injection, the NDFWM is operated up to a detuning range of 1.7 THz with a low injection ratio of 0.42. The normalized conversion efficiency (NCE) and the side-mode suppression ratio (SMSR) with respect to the converted signal are analyzed. The highest NCE of −17 dB associated with a SMSR of 20.3 dB is achieved at detuning of 110 GHz.

Index Terms: Quantum dot laser, injection locking, four-wave mixing.

1. Introduction

Optical wavelength conversion plays an important role in wavelength division multiplexed (WDM) systems. NDFWM in semiconductor gain media is a desirable technique for wavelength conversion due to its ultrafast nature and transparency to the modulation format of the signals [1], [2]. In addition, since the converted signal is the phase-conjugate replica of the input signal, it also provides the possibility for fiber dispersion compensation in long distance transmission systems [3], [4]. NDFWM in semiconductor optical amplifiers (SOAs) and distributed feedback (DFB) lasers have been extensively studied and much effort has been devoted to enhance the conversion efficiency (the ratio of the output-converted signal power to the input-signal power) and the optical signal-to-noise ratio [5]–[9]. Generally, the SOA has a larger linear gain, which provides high conversion efficiency, whereas it also generates additional amplified spontaneous emission noise. In this way, there is an optimum linear gain for the maximum conversion efficiency to noise ratio [5], while a compromise on the pump-wave power is also required to obtain a better performance [6]. In DFB lasers, the lasing mode itself is used as a pump wave, and the NDFWM is enhanced by the cavity resonance. A higher conversion efficiency associated with a lower noise level can be

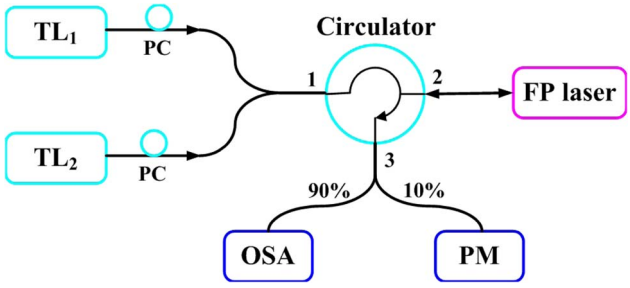

Fig. 1. Schematic of the experimental setup. $TL_{1,2}$: Tunable laser; PC: Polarization controller; OSA: Optical spectrum analyzer and PM: Power meter.

achieved from a laser with a long cavity and a small grating coupling coefficient. A high lasing power is also favorable for obtaining higher conversion efficiency [7]–[9]. As for the nonlinear gain medium, in contrast to the quantum well (QW) material, quantum dots (QDs) offer various advantages such as a wider gain spectrum [10], ultrafast carrier dynamics [11], higher nonlinear gain effect and thus a larger three-order nonlinear susceptibility [9], [12], [13]. In addition, due to the reduced linewidth enhancement factor (LEF), QDs have the possibility of eliminating destructive interference among the nonlinear processes and also offer an enhanced efficiency in the wavelength up-conversion [14], [15]. In order to improve the dynamical performance of semiconductor lasers, the optical injection-locking technique has been widely used to reduce the spectral linewidth, frequency chirp as well as to suppress relative intensity noise and nonlinear distortion [16]–[18]. In particular, it has been reported that the LEF value can be reduced under strong optical injection as well [19]–[21], which is quite beneficial for further suppressing the destructive interference. Employing a dual-mode injection-locking scheme in this work, we report the efficient NDFWM generation in a QD Fabry–Perot (FP) laser, in which one tone of the injected continuous-wave (CW) beams is used as the pump wave, while the other one plays the role of the probe wave. Each of these locks a longitudinal mode of the FP laser within the stable-locking range.

2. Experimental Setup

Fig. 1 shows the experimental setup, where two tunable CW lasers ($TL_{1,2}$: Yenista Optics, T100S) are injected into the QD laser via an optical circulator. The QD laser output is collected from port 3 of the circulator, which is followed by a 90/10 fiber splitter. The 10% port is connected with a power meter (PM) to monitor the output power while the 90% port is used to analyze the optical spectrum with an optical spectrum analyzer (OSA). The polarization of the tunable lasers is controlled to align with the slave laser through the polarization controller (PC). The temperature of the QD laser is kept constant at 293 K throughout the experiment using a thermo-electric cooler.

Fig. 2 illustrates the epi-layer structure of the QD laser. The QD structure was grown by gas source molecular beam epitaxy on a 2° misoriented (100) n-doped InP substrate. The mis-orientation allows the formation of QDs instead of quantum dashes which are traditionally formed on InP(100) oriented substrate [22]. The active layer consists of six stacked layers of InAs dots which are embedded in an InGaAsP quaternary alloy. The 4-μm wide ridge waveguide was fabricated by selective wet and dry etching sequence based on a CH_4-H_2-Ar RIE plasma using a Ti-Au mask. Then, a benzocyclobutene (BCB) layer was spin-coated to planarize the mesa structure and dry-etched back to expose the top surface of the ridge. This self-alignment step enables the p-contact electrode to be defined by Ti-Au e-beam evaporation. The substrate was thinned to 150 μm and a backside n-type metallization was performed with an AuGe sputtered alloy. Finally, the device was cleaved into a 830-μm long cavity.

3. Results and Discussions

Fig. 3(a) depicts the output power of the solitary QD laser coupled into a lensed optical fiber as a function of the pump current at room temperature. The laser exhibits a threshold current of about

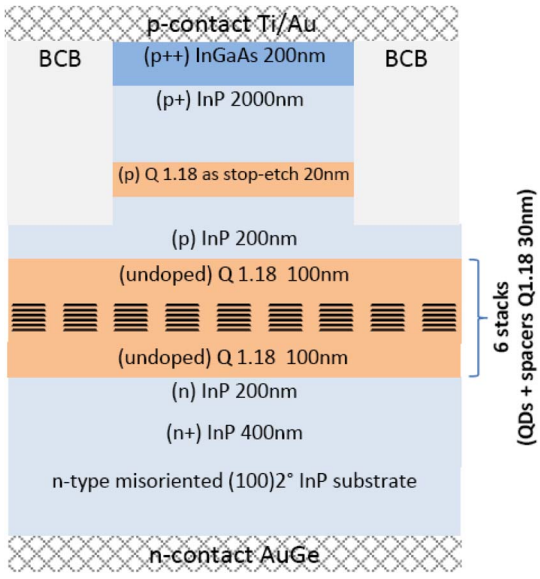

Fig. 2. The epi-layer structure of the InAs/InP(100) QD laser. "Q1.18" denotes that the quaternary alloy $In_{0.8}Ga_{0.2}As_{0.435}P_{0.565}$ emits at 1.18 μm. The stop-etch layer is used to control the etch depth. "BCB" denotes benzocyclobutene, and "+" or "++" indicates the doping level.

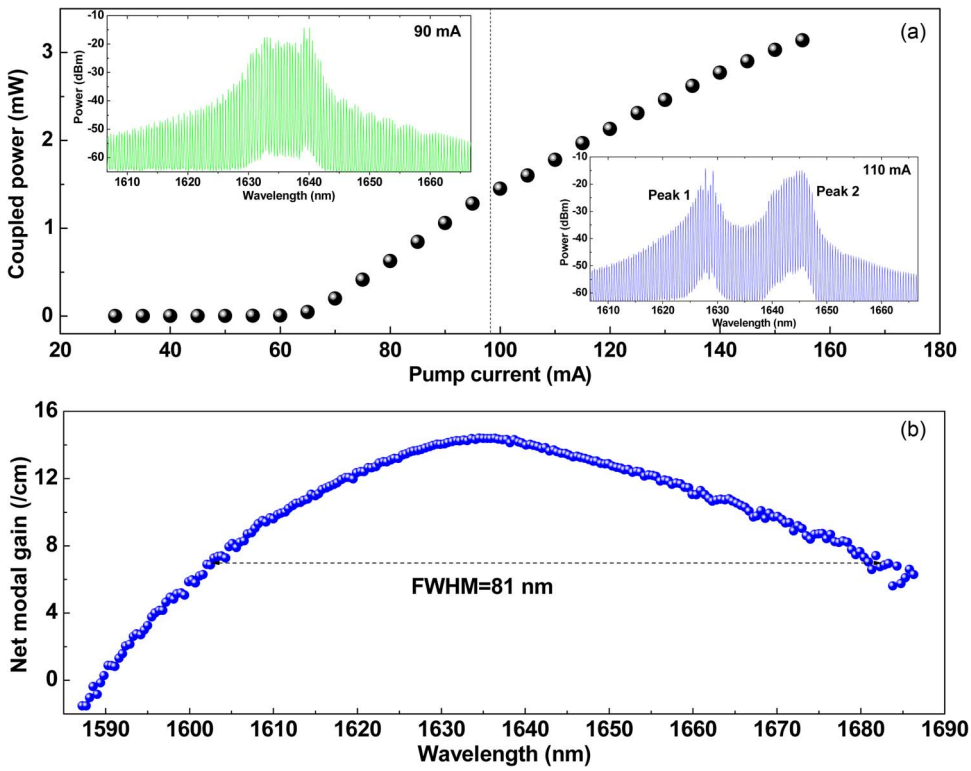

Fig. 3. (a) Light versus pump current, the dashed line indicates the onset of the optical spectrum split. Insets are the free-running spectra measured at 90 mA (green) and 110 mA (blue), respectively. (b) Sub-threshold net modal gain spectrum with a FWHM of 81 nm. The resolution of the OSA is set at 70 pm.

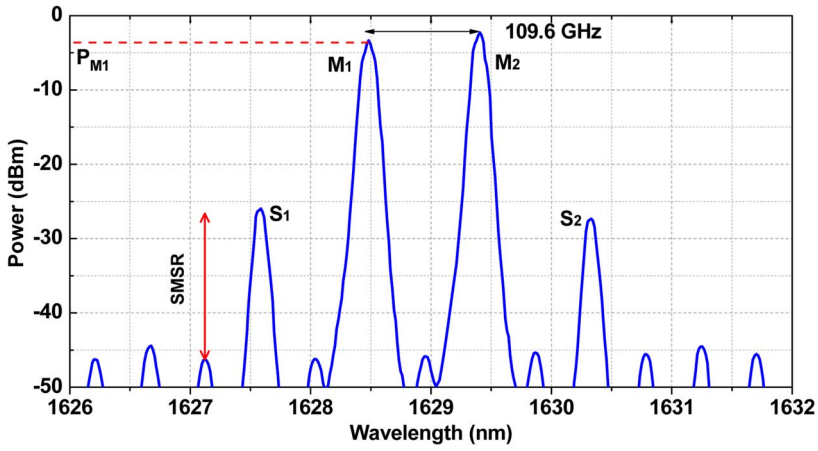

Fig. 4. Optical spectrum with FWM. $M_{1,2}$ are the stably locked modes by the tunable master lasers. The frequency difference between the locked modes is 109.6 GHz. $S_{1,2}$ are the newly converted signals.

64 mA. Interestingly, when the current increases above threshold, the free-running optical spectrum is broadened as shown in the inset (green) at 90 mA with a peak centered around 1635 nm, and then splits into two separated peaks above about 98 mA (dashed line). As an illustration, the spectral difference between the split peaks at 110 mA (blue) is 17 nm while it increases up to 23 nm at 160 mA. The phenomenon that the wavelength detuning varies as a function of the pump current is a specific feature of the QD material and has been already reported in [23]. The corresponding physical mechanism was attributed to the Rabi oscillation as well as to the state filling effect [23], [24]. It is noted that this typical feature observed in the optical spectrum does not result from the vertical electronic coupling of the QD multi-layers [25] or the separate excited state emission [26]. The wide split optical spectrum provides the possibility for the efficient generation of NDFWM with a wide tuning range. Employing the Hakki-Paoli method [27], the extracted net modal gain slightly below the threshold current is shown in Fig. 3(b). The gain spectrum exhibits a full-width at half maximum (FWHM) of about 81 nm and a maximum gain of 14.4 cm^{-1} at 1634.5 nm. Moreover, it has been shown that such a QD laser structure has the capability to reach an even higher material gain [28]. In the experimental study of the NDFWM performance, the QD laser is biased at 110 mA with a fiber-coupled power of 2.0 mW. Each of the two tunable lasers is set at the maximum achievable power around 1.4 mW (1.43 mW for TL_1 and 1.38 mW TL_2), which are measured at port 2 of the circulator. Assuming a power coupling efficiency of 60% [29], the injection ratio for each of the master lasers to the slave laser is calculated to be 0.42, meaning that the strength of the optical injection remains at a relatively low level. The wavelength of the master laser TL_1 is fixed around the center of peak 1 [inset of Fig. 3(a)] and acts as the pump wave, while TL_2 is tuned to a longer wavelength and acts as the probe wave.

Fig. 4 shows an optical spectrum of the dual-mode injection-locked QD laser. Each injected wavelength selects a longitudinal mode within the free-running FP multimodes, while all other modes are well suppressed. M_1 and M_2 are the stable locked modes by TL_1 and TL_2, respectively. Due to the third-order nonlinear susceptibility $\chi^{(3)}$, new waves S_1 and S_2 are generated as the converted conjugate signal of M_2 and M_1. Assuming the frequency difference between M_1 and M_2 is $\Delta f = f_{M1} - f_{M2}$, the FWM process is governed by the carrier density pulsation (CDP) mechanism for Δf within a few GHz [30], where the beating between the pump and probe waves creates temporal gain and index gratings. For larger frequency detunings up to THz range, spectral hole burning (SHB) and carrier heating (CH) dominates. In the SHB mechanism, the injected signals create a hole and change the intraband carrier distribution, producing a modulation of the occupation probability of carriers within the energy band [31]. In the case of QD lasers, the slow interdot processes on the order of a few to tens of picoseconds allow for the creation of deeper spectral holes and thus for more efficient FWM [11]. The CH mechanism is caused by the stimulated emission from the

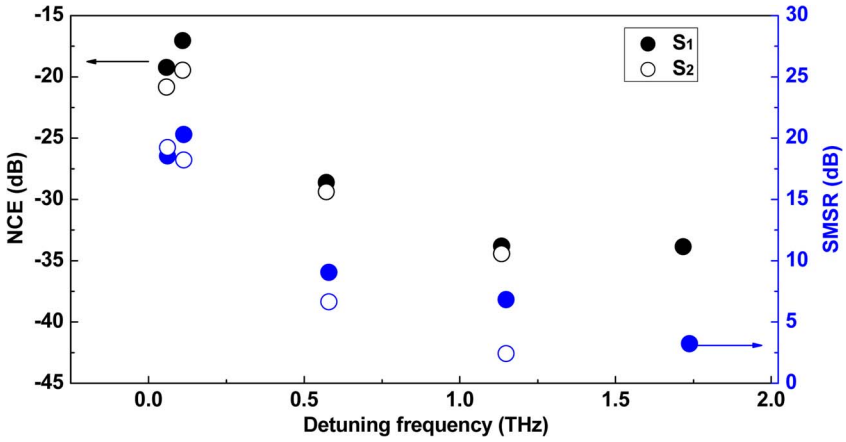

Fig. 5. The normalized conversion efficiency (NCE) η_{S1}, η_{S2} (black) and SMSR (blue) as a function of the detuning frequency. S_1 is denoted by the full circle, and S_2 is by the open circle. Note that signal S_2 at 1.72 THz is invisible because it is submerged in the residual FP modes.

ground state, which removes the lowest energy carriers, while free carriers absorb photons and increase the energy [11], [31]. The frequencies of the two newly generated signals respectively are $f_{S1} = f_{M1} + \Delta f$ and $f_{S2} = f_{M2} - \Delta f$. Then the corresponding susceptibilities are [14]:

$$\chi^{(3)}(f_{S_1}) = \sum_B \chi_B^{(3)}(\Delta f = 0)(1 - i2\pi\Delta f\tau_B)^{-1}$$
$$\chi^{(3)}(f_{S_2}) = \sum_B \chi_B^{(3)}(\Delta f = 0)(1 + i2\pi\Delta f\tau_B)^{-1} \quad (1)$$

where B denotes the contributions from SHB, CH and CDP, and τ_B is the corresponding time constant. The electric field of the FWM signal is proportional to the induced polarization $D(f)$ [32]:

$$D(f_{S_1}) = \varepsilon_0\chi^{(3)}(f_{S_1})E^2(f_{M_1})E^*(f_{M_2}) \quad D(f_{S_2}) = \varepsilon_0\chi^{(3)}(f_{S_2})E^2(f_{M_2})E^*(f_{M_1}). \quad (2)$$

The normalized conversion efficiency (NCE) is then found to be [33]:

$$\eta_{S1} = \frac{P_{S1}}{P_{M1}^2 P_{M2}} \qquad \eta_{S2} = \frac{P_{S2}}{P_{M2}^2 P_{M1}} \quad (3)$$

where $P_X(X = M_{1,2}, S_{1,2})$ is the corresponding wave output power, which can be extracted from the optical spectrum. Following this definition, the normalized conversion efficiency (black) of the FWM in the QD laser is presented in Fig. 5. The interval of the detuning frequency Δf is mainly determined by the mode spacing, which is 0.46 nm in the QD laser under study. The detuning frequency is then operated from the minimum 57.6 GHz up to 1.72 THz. For even larger detunings up to 5.7 THz, the FWM signal is submerged in the residual FP modes or noise and disappears. Due to the asymmetric gain spectrum as shown in Fig. 3(b) and carrier populations in higher energy non-lasing states, the QD laser has a non-zero LEF parameter [34]. By extracting the differential gain and the wavelength drift with the pump current, the measured below-threshold LEF of the laser device under study is found to be 2.6 at 1625 nm. Representing the susceptibilities $\chi_{CDP}^{(3)}$, $\chi_{SHB}^{(3)}$ and $\chi_{CH}^{(3)}$ as complex phasors [14], it is found that this finite LEF value causes the phasors to be oriented in different directions at zero detuning. When the frequency difference is tuned, on one hand $\chi_{CDP}^{(3)}$ begins to rotate and its direction becomes closer to that of $\chi_{SHB}^{(3)}$ and $\chi_{CH}^{(3)}$. On the other hand, the magnitude of each susceptibility becomes smaller as expressed in equation (1). Then η increases and reaches the peak value when the norm of the three additive susceptibilities is the largest. In the experiment under study, this situation is achieved at the detuning frequency $\Delta f = 109.6$ GHz with a normalized conversion efficiency of -17 dB (η_{S1}). Beyond that, the direction of $\chi_{CDP}^{(3)}$ deviates away

and the conversion efficiency decreases with the detuning frequency. When Δf is tuned above the characteristic rates (1 THz) of the SHB and CH processes, $\chi^{(3)}_{SHB}$ and $\chi^{(3)}_{CH}$ also begin to rotate making η nearly constant at about -34 dB from $\Delta f = 1.13$ THz to 1.72 THz in the experiment. It is noted that at a detuning frequency around 1.1 THz, the NCE of the studied QD laser is more than 15 dB larger than that of a QW SOA reported in [33]. From equations (1)–(3), it can be derived that $\eta_{S1} = \eta_{S2}$. However, the experimental results depicted in Fig. 5 show that η_{S2} is slightly smaller than η_{S1}, which is attributed to the assertion that the SHB effect contributes less to the wavelength up-conversion [35]. In addition, Fig. 5 also presents the variation of SMSR (blue) with respect to each converted signal S_1 and S_2 since the residual modes act as optical noise to the converted signals. The SMSR decreases with the detuning frequency and the highest ratio is 20.3 dB at $\Delta f = 109.6$ GHz. The SMSR of S_2 is smaller in comparison with S_1, which can be partly attributed to the lower power of S_2. On the other hand, the amplitude of the residual FP modes at the longer wavelength side is higher when the laser is injection locked. This is because the gain at the right side of the pump wave M_1 is larger than that at the left side. Since the gain spectrum is almost clamped above threshold [36], this trend can be partially reflected by the sub-threshold gain shown in Fig. 3(b).

Lastly, it is important to note that in the experiment both the pump wave and the probe signal are operated in the stable-locked regime. However, for an arbitrary probe wavelength the temperature of the FP laser can be controlled to tune one of the FP modes within the stable-locking range of the probe signal. In addition, because the converted signal is enhanced by the cavity resonance, it is important to make the converted signal coincide with one of the resonance frequency peaks in the laser cavity [37]. This can be achieved by tuning the pump wave since it typically has a large power and thus a wide locking range. Furthermore, the normalized conversion efficiency can be enhanced by a larger bias current to the FP laser, since the output power is mainly determined by the slave laser. The SMSR can be improved by a higher injection ratio [37], which can be achieved by coupling an amplifier into the configuration to amplify the pump wave power. Unfortunately, the impact of the injection strength on the FWM was not studied in this work due to the power limitation of the devices, which will be fulfilled in a following study.

4. Conclusion

In conclusion, we have experimentally investigated the NDFWM in a U-band QD FP laser employing the dual-mode injection-locking technique. Taking advantage of the two-peak lasing features of the free-running laser, efficient NDFWM is demonstrated from a detuning of 58 GHz up to 1.7 THz under a weak optical injection level. The performance can be further enhanced by increasing the FP laser bias current and by a higher injection ratio of the pump wave, which will require further investigation in the future. These results are of prime importance for the wavelength conversion technique in high-speed WDM systems as well as for the microwave signal generation and radio-over-fiber applications.

Acknowledgment

The authors would like to thank Prof. A. Le Corre from INSA-Rennes for providing the QD lasers, Prof. P. Gallion from Télécom ParisTech for the helpful discussions, and Dr. M. T. Crowley from Tyndall National Institute for his valuable comments.

References

[1] M. C. Tatham, G. Sherlock, and L. D. Westbrook, "20-nm optical wavelength conversion using nondegenerate four-wave mixing," *IEEE Phonon. Technol. Lett.*, vol. 5, no. 11, pp. 1303–1306, Nov. 1993.

[2] D. F. Geraghty, R. B. Lee, M. Verdiell, M. Ziari, A. Mathur, and K. J. Vahala, "Wavelength conversion for WDM communication systems using four-wave mixing in semiconductor optical amplifiers," *IEEE J. Sel. Topics Quantum Electron.*, vol. 3, no. 5, pp. 1146–1155, Oct. 1997.

[3] M. C. Tatham, X. Gu, L. D. Westbrook, G. Sherlock, and D. M. Spirit, "Transmission of 10 Gbit/s directly modulated DFB signals over 200 km standard fibre using mid-span spectral inversion," *Electron. Lett.*, vol. 30, no. 16, pp. 1335–1336, Aug. 1994.

[4] D. D. Marcenac, D. Nesset, A. E. Kelly, M. Brierly, A. D. Elllis, D. G. Moodie, and C. W. Ford, "40 Gbit/s transmission over 406 km of NDSF using mid-span spectral inversion by four-wave mixing in a 2 mm long semiconductor optical amplifier," *Electron. Lett.*, vol. 33, no. 10, pp. 879–880, May 1997.
[5] H. J. Kim, H. J. Song, and J. I. Song, "All-optical frequency up-conversion technique using four-wave mixing in semiconductor optical amplifiers for radio-over-fiber applications," in *Proc. IEEE/MTT-S Int. Microw. Symp.*, Jun. 2007, pp. 67–70.
[6] A. D'Ottavi, F. Martelli, P. Spano, A. Mecozzi, S. Scotti, R. D'Ara, J. Eckner, and G. Guekos, "Very high efficiency four-wave mixing in a single semiconductor traveling wave amplifier," *Appl. Phys. Lett.*, vol. 68, no. 16, pp. 2186–2188, Apr. 1996.
[7] T. Simoyama, H. Kuwatsuka, and H. Ishikawa, "Cavity length dependence of wavelength conversion efficiency of four-wave mixing in $\lambda/4$-shifted DFB laser," *FUJISU Sci. Tech. J.*, vol. 34, no. 2, pp. 235–244, Dec. 1998.
[8] H. J. Kim and J. I. Song, "All-optical frequency downconversion technique utilizing a four-wave mixing effect in a single semiconductor optical amplifier for wavelength division multiplexing radio-over-fiber applications," *Opt. Exp.*, vol. 20, no. 7, pp. 8047–8054, Mar. 2012.
[9] H. Su, H. Li, L. Zhang, Z. Zou, A. L. Gray, R. Wang, P. M. Varangis, and L. F. Lester, "Nondegenerate four-wave mixing in quantum dot distributed feedback lasers," *IEEE Photon. Technol. Lett.*, vol. 17, no. 8, pp. 1686–1688, Aug. 2005.
[10] H. Li, G. T. Liu, P. M. Varangis, T. C. Newell, A. Stintz, B. Fuchs, K. J. Malloy, and L. F. Lester, "150-nm tuning range in a grating-coupled external cavity quantum-dot laser," *IEEE Photon. Technol. Lett.*, vol. 12, no. 7, pp. 759–761, Jul. 2000.
[11] D. Nielsen and S. L. Chuang, "Four-wave mixing and wavelength conversion in quantum dots," *Phys. Rev. B*, vol. 81, no. 3, p. 035305, Jan. 2010.
[12] T. Akiyama, O. Wada, H. Kuwatsuka, T. Simoyama, Y. Nakata, K. Mukai, M. Sugawara, and H. Ishikawa, "Nonlinear processes responsible for nondegenerate four-wave mixing in quantum-dot optical amplifiers," *Appl. Phys. Lett.*, vol. 77, no. 12, pp. 1753–1755, Sep. 2000.
[13] Z. G. Lu, J. R. Liu, S. Raymond, P. J. Poole, P. J. Barrios, D. Poitras, F. G. Sun, G. Pakulski, P. J. Bock, and T. Hall, "Highly efficient non-degenerate four-wave mixing process in InAs/InGaAsP quantum dots," *Electron. Lett.*, vol. 42, no. 19, pp. 1112–1113, Sep. 2006.
[14] T. Akiyama, H. Kuwatsuka, N. Hatori, Y. Nakata, H. Ebe, and M. Sugawara, "Symmetric highly efficient ($\sim$0 dB) wavelength conversion based on four-wave mixing in quantum dot optical amplifiers," *IEEE Photon. Technol. Lett.*, vol. 14, no. 8, pp. 1139–1141, Aug. 2002.
[15] A. H. Flayyih and A. H. Al-Khursan, "Four-wave mixing in quantum dot semiconductor optical amplifiers," *Appl. Opt.*, vol. 52, no. 14, pp. 3156–3165, May 2013.
[16] G. Yabre, "Effect of relatively strong light injection on the chirp-to-power ratio and the 3 dB bandwidth of directly modulated semiconductor lasers," *J. Lightw. Tech.*, vol. 14, no. 10, pp. 2367–2373, Oct. 1996.
[17] T. B. Simpson, J. M. Liu, and A. Gavrielides, "Bandwidth enhancement and broadband noise reduction in injection-locked semiconductor lasers," *IEEE Photon. Technol. Lett.*, vol. 7, no. 7, pp. 709–711, Jul. 1995.
[18] X. J. Meng, T. Chau, and M. C. Wu, "Improved intrinsic dynamic distortions in directly modulated semiconductor lasers by optical injection locking," *IEEE Trans. Microw. Theory Tech.*, vol. 47, no. 7, pp. 1172–1176, Jul. 1999.
[19] N. A. Naderi, M. C. Pochet, F. Grillot, A. Shirkhorshidian, V. Kovanis, and L. F. Lester, "Manipulation of the linewidth enhancement factor in an injection-locked quantum-dash Fabry-Perot laser at 1550 nm," in *Proc. 23rd Annu. Meet. IEEE Photon. Soc.*, Nov. 2010, pp. 427–428.
[20] B. Lingnau, K. Ludge, W. W. Chow, and E. Scholl, "Failure of theα factor in describing dynamical instabilities and chaos in quantum-dot lasers," *Phys. Rev. E*, vol. 86, no. 6, pp. 065201-1–065201-5, Dec. 2012.
[21] C. H. Lin and F. Y. Lin, "Four-wave mixing analysis on injection-locked quantum dot semiconductor lasers," *Opt. Exp.*, vol. 21, no. 18, pp. 21242–21253, Sep. 2013.
[22] F. Lelarge, B. Dagens, J. Renaudier, R. Brenot, A. Accard, F. Van Dijk, D. Make, O. Le Gouezigou, J. Provost, F. Poingt, J. Landreau, O. Drisse, E. Derouin, B. Rousseau, F. Pommereau, and G.-H. Duan, "Semiconductor lasers and optical amplifiers operating at 1.55μm," *IEEE J. Sel. Top. Quantum. Electron.*, vol. 13, no. 1, pp. 111–124, Jan./Feb. 2007.
[23] S. G. Li, Q. Gong, Y. F. Lao, H. D. Yang, S. Gao, P. Chen, Y. G. Zhang, S. L. Feng, and H. L. Wang, "Two-color quantum dot laser with tunable wavelength gap," *Appl. Phys. Lett.*, vol. 95, no. 25, pp. 251 111–251 113, Dec. 2009.
[24] T. H. Stievater, X. Q. Li, D. G. Steel, D. Gammon, D. S. Katzer, D. Park, C. Piermarocchi, and L. J. Sham, "Rabi oscillations of excitons in single quantum dots," *Phys. Rev. Lett.*, vol. 87, no. 13, pp. 133 603–133 606, Sep. 2001.
[25] P. Miska, J. Even, C. Paranthoen, O. Dehaese, A. Jbeli, M. Senès, and X. Marie, "Vertical electronic coupling between InAs/InP quantum-dot layers emitting in the near-infrared range," *Appl. Phys. Lett.*, vol. 86, no. 11, pp. 111 905–111 907, Mar. 2005.
[26] C. Cornet, A. Schliwa, J. Even, C. Cornet, A. Schliwa, J. Even, F. Doré, C. Celebi, A. Létoublon, E. Macé, C. Paranthoën, A. Simon, P. M. Koenraad, N. Bertru, D. Bimberg, and S. Loualiche, "Electronic and optical properties of InAs/InP quantum dots on InP(100) and InP(311)B substrates: Theory and experiment," *Phys. Rev. B*, vol. 74, no. 3, p. 3035312, Jul. 2006.
[27] R. Raghuraman, N. Yu, R. Engelmann, H. Lee, and C. L. Shieh, "Spectral dependence of differential gain, mode shift, and linewidth enhancement factor in a InGaAs-GaAs strained-layer single-quantum-well laser operated under high-injection conditions," *IEEE J. Quantum Electron.*, vol. 29, no. 1, pp. 69–75, Jan. 1993.
[28] C. Cornet, C. Labbé, H. Folliot, N. Bertru, O. Dehaese, J. Even, A. Le Corre, C. Paranthoen, C. Platz, and S. Loualiche, "Quantitative investigation of optical absorption in InAs/InP (311)B quantum dots emitting at 1.55 μm wavelength," *Appl. Phys. Lett.*, vol. 85, no. 23, pp. 5685–5687, Oct. 2004.
[29] N. A. Naderi, M. Pochet, F. Grillot, N. B. Terry, V. Kovanis, and L. F. Lester, "Modeling the injection-locked behavior of a quantum dash semiconductor laser," *IEEE J. Sel. Topics Quantum Electron.*, vol. 15, no. 3, pp. 563–571, Jun. 2009.
[30] G. P. Agrawal, "Population pulsations and nondegenerate four-wave mixing in semiconductor lasers and amplifiers," *J. Opt. Soc. Amer. B*, vol. 5, no. 1, pp. 147–159, Jan. 1988.

[31] K. Kikuchi, M. Kakui, C. E. Zah, and T. P. Lee, "Observation of highly nondegenerate four-wave mixing in 1.5 μm traveling-wave semiconductor optical amplifiers and estimation of nonlinear gain coefficient," *IEEE J. Quantum Electron.*, vol. 28, no. 1, pp. 151–156, Jan. 1992.
[32] I. Park, I. Fischer, and W. Elsäer, "Highly nondegenrate four-wave mixing in a tunable dual-mode semiconductor laser," *Appl. Phys. Lett.*, vol. 84, no. 25, pp. 5189–5191, Jun. 2004.
[33] I. Koltchanov, S. Kindt, K. Petermann, S. Diez, R. Ludwig, R. Schnabel, and H. G. Weber, "Analytical theory of terahertz four-wave mixing in semiconductor-laser amplifiers," *Appl. Phys. Lett.*, vol. 68, no. 20, pp. 2787–2789, Mar. 1996.
[34] F. Grillot, B. Dagens, J. G. Provost, H. Su, and L. F. Lester, "Gain compression and above-threshold linewidth enhancement factor in 1.3 μm InAs-GaAs quantum-dot lasers," *IEEE J. Quantum Electron.*, vol. 44, no. 10, pp. 946–951, Oct. 2008.
[35] A. D'Ottavi, E. Iannone, A. Mecozzi, S. Scotti, P. Spano, J. Landreau, A. Ougazzaden, and J. C. Bouley, "Investigation of carrier heating and spectral hole burning in semiconductor amplifiers by highly nondegenerate four-wave mixing," *Appl. Phys. Lett.*, vol. 64, no. 19, pp. 2492–2494, May 1994.
[36] M. Gioannini, A. Sevega, and I. Montrosset, "Simulations of differential gain and linewidth enhacement factor of quantum dot semiconductor lasers," *Opt. Quantum Electron.*, vol. 38, no. 4–6, pp. 381–394, Jan. 2006.
[37] L. L. Li and K. Petermann, "Small-signal analysis of THz optical-frequency conversion in an injection-locked semiconductor laser," *IEEE J. Quantum. Electron.*, vol. 29, no. 12, pp. 2988–2994, Dec. 1993.